Available online at www.sciencedirect.com

ScienceDirect

Nuclear Physics A 982 (2019) 515–518

NUCLEAR PHYSICS A

www.elsevier.com/locate/nuclphysa

XXVIIth International Conference on Ultrarelativistic Nucleus-Nucleus Collisions (Quark Matter 2018)

Spin alignment measurements using vector mesons with ALICE detector at the LHC

Ranbir Singh (For the ALICE Collaboration)

School of Physical Sciences, National Institute of Science Education and Research, HBNI, Jatni-752050, India

Abstract

We present new measurements related to spin alignment of K^{*0} vector mesons at mid-rapidity for Pb–Pb collisions at $\sqrt{s_{\mathrm{NN}}}$ = 2.76 and 5.02 TeV. The spin alignment measurements are carried out with respect to production plane and 2^{nd} order event plane. At low p_{T} the spin density matrix element ρ_{00} for K^{*0} is found to have values slightly below 1/3, while it is consistent with 1/3, i.e. no spin alignment, at high p_{T} . Similar values of ρ_{00} are observed with respect to both production plane and event plane. Within statistical and systematic uncertainties, ρ_{00} values are also found to be independent of $\sqrt{s_{\mathrm{NN}}}$. ρ_{00} also shows centrality dependence with maximum deviation from 1/3 for mid-central collisions with respect to both the kinematic planes. The measurements for K^{*0} in pp collisions at $\sqrt{s}$ = 13 TeV and for $\mathrm{K}^0_{\mathrm{S}}$ (a spin 0 hadron) in 20-40% central Pb–Pb collisions at $\sqrt{s_{\mathrm{NN}}}$ = 2.76 TeV are consistent with no spin alignment.

Keywords: heavy-ion collision, spin alignment, vector meson, ALICE

1. Introduction

Relativistic heavy-ion collisions are expected to produce quark gluon plasma with large angular momentum [1] and intense magnetic field [2]. One of the main goals of the ALICE physics program in heavy-ion collisions is to look for the signatures of these effects. The proposed signature is the measurement of the spin alignment of vector mesons. The spin alignment measurements can be performed by studying the angular distributions of the vector meson decay daughters [3, 4, 5]. The angular distribution of vector mesons [6] is given by

$$\frac{\mathrm{d}N}{\mathrm{d}\cos\theta^*} = N_0[(1-\rho_{00}) + \frac{1}{R}\cos^2\theta^*(3\rho_{00}-1)], \tag{1}$$

where N_0 is a normalization constant. θ^* is the angle formed by one of the vector meson decay daughters in the rest frame of the vector meson with the quantization axis or polarization direction. The quantization axis can be normal to the production plane, that is determined by the momentum of the vector meson and the beam direction. It can also be normal to the reaction plane that is determined by the impact parameter and the beam direction. R is the event plane resolution. In case of the production plane analysis R = 1. ρ_{00} is the zeroth element of the spin density matrix, which is a 3x3 hermitian matrix with unit trace. Since K^{*0} decays

https://doi.org/10.1016/j.nuclphysa.2018.12.004
0375-9474/© 2018 Published by Elsevier B.V.

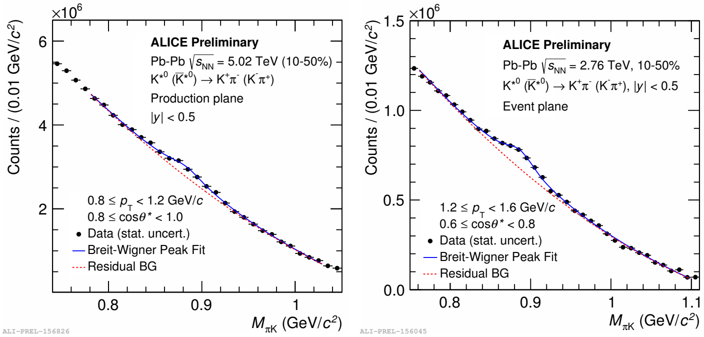

Fig. 1. (color online) Left panel: Invariant mass distribution of πK pairs at mid-rapidity after combinatorial background subtraction w.r.t. the production plane for 10-50% central Pb–Pb collisions at $\sqrt{s_{\rm NN}}$ = 5.02 TeV. Right panel: Invariant mass distribution of πK pairs at mid-rapidity after combinatorial background subtraction w.r.t. the event plane in 10-50% central Pb–Pb collisions at $\sqrt{s_{\rm NN}}$ = 2.76 TeV. The invariant mass distributions are fitted with a Breit-Wigner function for the signal and a second-order polynomial function in $M_{\pi {\rm K}}$ for the residual background. The error bars are statistical only.

via the strong interaction, the diagonal elements ρ_{11} and ρ_{-1-1} are degenerate and the only independent observable is ρ_{00} . The polarization effects caused by either initial conditions or final state effects would lead to non-uniform angular distributions of vector mesons. This results in a deviation of the ρ_{00} from 1/3, which indicates a net spin alignment whereas ρ_{00} = 1/3 signals no spin alignment. Here we present new results related to the spin alignment of K^{*0} vector mesons in Pb–Pb collisions at $\sqrt{s_{\rm NN}}$ = 2.76 and 5.02 TeV measured as a function of $p_{\rm T}$ and centrality. The spin density matrix element ρ_{00} is measured w.r.t. the production and event planes using the ALICE detector [7].

2. Analysis details

In this work we have measured the spin alignment of K^{*0} at mid-rapidity ($|y| < 0.5$) in Pb–Pb collisions at $\sqrt{s_{\rm NN}}$ = 2.76 and 5.02 TeV in various collision centrality classes. The analysis is carried out using 14 M minimum bias events in Pb–Pb collisions at $\sqrt{s_{\rm NN}}$ = 2.76 TeV collected in 2010 and 30 M minimum bias events in Pb–Pb collisions at $\sqrt{s_{\rm NN}}$ = 5.02 TeV collected in 2015. The spin alignment results for K^{*0} in pp collisions at $\sqrt{s}$ = 13 TeV, as a baseline study, and of K^0_S (a spin 0 hadron) in 20-40% central Pb–Pb collisions at $\sqrt{s_{\rm NN}}$ = 2.76 TeV, as null hypothesis, are reported in [8]. The spin alignment study of K^{*0} is performed w.r.t. the production and event planes, but the event plane analysis is performed in Pb–Pb collisions at $\sqrt{s_{\rm NN}}$ = 2.76 TeV only. The detectors that are used for this analysis are Time Projection Chamber (TPC) and Time-Of-Flight (TOF) detector for particle identification at mid-rapidity and the forward detector V0 for triggering and centrality estimation. The V0 detector is also used for the estimation of the 2^{nd} order event plane having a typical resolution of 0.70 for 10-50% centrality class. The K^{*0} vector meson is reconstructed through the invariant mass of its decay daughters from its dominant hadronic decay channel ($K^{*0} \rightarrow K^{\pm}\pi^{\mp}$). The major contribution to the background in the invariant mass distributions is combinatorial. It is estimated using the mixed event technique, where opposite charged K and π from different events are mixed. These events are required to have similar multiplicity and collision point position. Even after subtracting combinatorial background still a certain amount of residual background remains under the resonance peak that is described by the second-order polynomial in this analysis. The invariant mass distributions of πK pairs, after combinatorial background subtraction, are shown in Fig. 1 for Pb–Pb collisions. These are the representative plots shown for a particular $p_{\rm T}$ and $\cos\theta^*$ bin and the same procedure is followed for each $p_{\rm T}$ and $\cos\theta^*$ bin of the analysis. These distributions are then fitted with a Breit-Wigner function for the signal and a second-order polynomial for the residual background to extract the K^{*0} yield in each $p_{\rm T}$ and $\cos\theta^*$ bin of a particular centrality class. The K^{*0} yields are then corrected for the corresponding reconstruc-

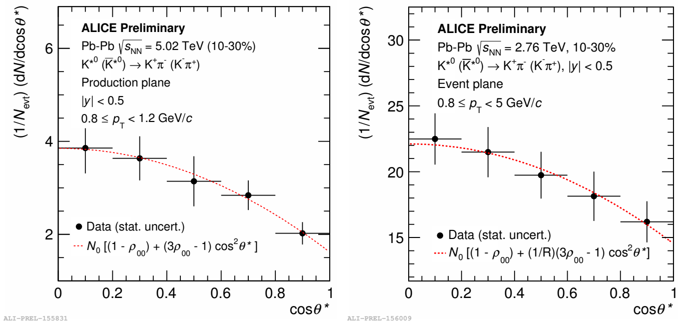

Fig. 2. (color online) Left panel: $dN/d\cos\theta^*$ vs. $\cos\theta^*$ at mid-rapidity w.r.t. the production plane for 10-30% central Pb–Pb collisions at $\sqrt{s_{NN}}$ = 5.02 TeV. Right panel: $dN/d\cos\theta^*$ vs. $\cos\theta^*$ at mid-rapidity w.r.t. the event plane for 10-30% central Pb–Pb collisions at $\sqrt{s_{NN}}$ = 2.76 TeV. The error bars are statistical only.

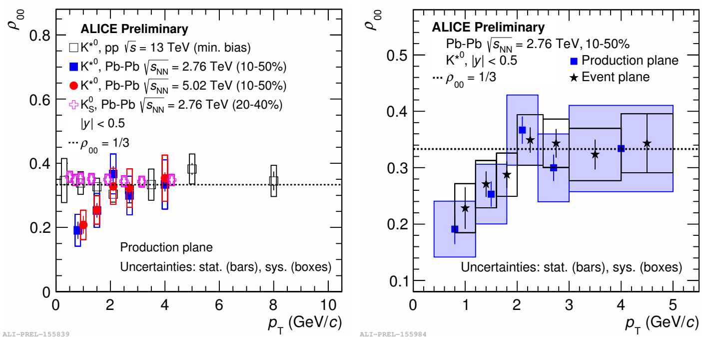

Fig. 3. (color online) Left panel: ρ_{00} vs. p_T of K^{*0} w.r.t. the production plane in pp collisions at $\sqrt{s}$ = 13 TeV and for 10-50% Pb–Pb collisions at $\sqrt{s_{NN}}$ = 2.76 and 5.02 TeV. The corresponding results for K^0_S , a spin zero hadron, for 20-40% Pb–Pb collisions at $\sqrt{s_{NN}}$ = 2.76 TeV are also shown. Right panel: Comparison of ρ_{00} w.r.t. production and event planes in Pb–Pb collisions at $\sqrt{s_{NN}}$ = 2.76 TeV. The statistical uncertainties are shown as bars and systematic uncertainties are shown as boxes. The dotted line at ρ_{00} = 1/3 shows the no spin alignment scenario.

tion efficiency and acceptance evaluated using dedicated Monte Carlo simulations [9, 10]. The left panel of Fig. 2 shows the $dN/d\cos\theta^*$ distribution at mid-rapidity, corrected for efficiency and acceptance, for $0.8 \leq p_T < 1.2$ GeV/c in 10-30% central Pb–Pb collisions at $\sqrt{s_{NN}}$ = 5.02 TeV using the production plane. The right panel shows the same distribution for $0.8 \leq p_T < 5.0$ GeV/c in 10-30% central Pb–Pb collisions at $\sqrt{s_{NN}}$ = 2.76 TeV using the event plane. The red dotted lines in the plots are fits with the functional form reported in Eq. 1. The ρ_{00} values for each p_T bin in various centrality classes are extracted from the fits.

3. Results

The left panel of Fig. 3 shows ρ_{00} as a function of p_T for K^{*0} in pp collisions at $\sqrt{s}$ = 13 TeV, in 10-50% Pb–Pb collisions at $\sqrt{s_{NN}}$ = 2.76 and 5.02 TeV and K^0_S in 20-40% Pb–Pb collisions at $\sqrt{s_{NN}}$ = 2.76 TeV using the production plane. A comparison of K^{*0} results using the production and event planes in Pb–Pb collisions at $\sqrt{s_{NN}}$ = 2.76 TeV is shown in the right panel of Fig. 3. The K^{*0} results in pp collisions and K^0_S (spin 0) in Pb–Pb collisions are almost consistent with 1/3, indicating no spin alignment. The ρ_{00} values of K^{*0} are lower than 1/3 at low p_T (< 2.0 GeV/c) for both production and event planes. The significance of ρ_{00} value of K^{*0} for $0.4 \leq p_T < 1.2$ GeV/c is about 2.5σ lower than 1/3 and about 2.3σ lower than

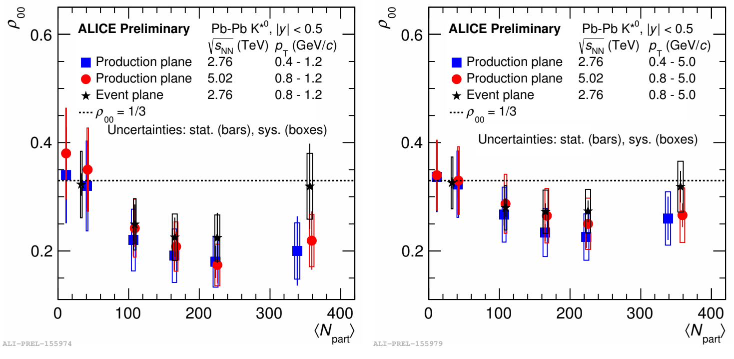

Fig. 4. (color online) Spin density matrix element ρ_{00} of K^{*0} as a function of $\langle N_{\rm part}\rangle$ w.r.t. production plane in Pb–Pb collisions at $\sqrt{s_{\rm NN}}$ = 2.76 TeV (blue marker) and 5.02 TeV (red marker) and w.r.t. event plane (black marker) in Pb–Pb collisions at $\sqrt{s_{\rm NN}}$ = 2.76 TeV for the lowest $p_{\rm T}$ bin (left panel) and for the whole $p_{\rm T}$ range (right panel). The statistical uncertainties are shown as bars and systematic uncertainties are shown as boxes. The dotted line at ρ_{00} = 1/3 shows the no spin alignment scenario.

1/3 for 0.8 ≤ $p_{\rm T}$ < 1.2 GeV/c using the production plane in Pb–Pb collisions at $\sqrt{s_{\rm NN}}$ = 2.76 and 5.02 TeV, respectively. The ρ_{00} value for K^{*0} at 0.8 ≤ $p_{\rm T}$ < 1.2 GeV/c using event plane in Pb–Pb collisions at $\sqrt{s_{\rm NN}}$ = 2.76 TeV is about 1.7σ lower than 1/3. The ρ_{00} values for K^{*0} are consistent with 1/3 for higher $p_{\rm T}$ at both energies w.r.t. the production and event planes. Figure 4 shows ρ_{00} as a function of $\langle N_{\rm part}\rangle$ in Pb–Pb collisions for the lowest $p_{\rm T}$ bin used in this analysis (left panel) and for the whole $p_{\rm T}$ range (right panel). ρ_{00} values show a clear centrality dependence in Pb–Pb collisions for both production and event planes. The maximum deviation of ρ_{00} values from 1/3 is for mid-central (10-30%) collisions that is expected due to the large angular momentum for mid-central collisions. Within statistical and systematic uncertainties the ρ_{00} values do not show energy dependence and similar values are observed both for production and event planes.

4. Summary and outlook

We have presented results on the spin alignment of K^{*0} vector mesons at mid-rapidity in Pb–Pb collisions at $\sqrt{s_{\rm NN}}$ = 2.76 and 5.02 TeV. The spin alignment is measured as a function of $p_{\rm T}$ and collision centrality classes with respect to the production and event planes. At low $p_{\rm T}$ (< 2.0 GeV/c) the ρ_{00} values deviate from 1/3 for both the production and event planes. Within statistical and systematic uncertainties the spin alignment results show no energy dependence. ρ_{00} shows a clear centrality dependence for both the kninematic planes and the maximum deviation of ρ_{00} from no spin alignment value 1/3 is observed for mid-central (10-30%) collisions. The spin alignment studies of K^{*0} with respect to the event plane in Pb–Pb collisions at $\sqrt{s_{\rm NN}}$ = 5.02 TeV is ongoing. Furthermore, an increase in statistical precision is expected with more data in Pb–Pb collisions at $\sqrt{s_{\rm NN}}$ = 5.02 TeV.

References

[1] F. Becattini, F. Piccinini and J. Rizzo, Phys. Rev. C **77**, 024906 (2008).
[2] D. E. Kharzeev, L. D. McLerran and H. J. Warringa, Nucl. Phys. A **803**, 227 (2008).
[3] B. I. Abelev *et al.* [STAR Collaboration], Phys. Rev. C **76**, 024915 (2007).
[4] L. Adamczyk *et al.* [STAR Collaboration], Nature **548**, 62 (2017).
[5] B. I. Abelev *et al.* [STAR Collaboration], Phys. Rev. C **77**, 061902 (2008).
[6] K. Schilling, P. Seyboth and G. E. Wolf, Nucl. Phys. B **15**, 397 (1970).
[7] B. Abelev *et al.* [ALICE Collaboration], Int. J. Mod. Phys. A **29**, 1430044 (2014).
[8] B. Mohanty [ALICE Collaboration] SQM 2017 proceeding, EPJ Web of Conferences 171, 16008 (2018).
[9] J. Adam *et al.* [ALICE Collaboration], Phys. Rev. C **95**, no. 6, 064606 (2017).
[10] B. Abelev *et al.* [ALICE Collaboration], Phys. Rev. C **91**, 024609 (2015).